Radio Science, Volume 35, Number 6, Pages 1389–1398, November–December 2000

Effects of humidity and precipitation on VHF radar vertical beam echoes

G. Vaughan and R. M. Worthington[1]

Department of Physics, University of Wales, Aberystwyth

Abstract. We investigate in this paper the variation in power of VHF radar vertical echoes as a function of atmospheric humidity. We find that the echoes are greatest in air of moderate (30-70%) humidity, and least in very dry or near-saturated air. Compared to moderate humidities, the standard model for radar echoes, based on potential refractivity, overpredicts the echo power at high relative humidity by ~10 dB. We propose that this is due to the effect of precipitation in suppressing small-scale humidity gradients. A model which assumes complete suppression underpredicts the observed power drastically, showing that precipitation can only remove a part of the small-scale structure in refractivity which is caused by fluctuations in humidity.

1. Introduction

The ability of a VHF radar to measure continuous profiles throughout the troposphere and lower stratosphere of winds, echo power, and turbulence in all weather conditions makes it an invaluable tool for research in mesoscale meteorology. Observations of frontal passages were presented by *Röttger* [1979], *Shapiro et al.* [1984] and *Larsen and Röttger* [1985]; the increase in static stability in the front causes a local maximum in radar reflectivity which allows the radar to track it. This technique is particularly suitable for locating upper tropospheric features; low-level fronts are best identified from the associated wind shear [*May et al.*, 1991] since the low-altitude radar reflectivity is dominated by humidity gradients which are not correlated with the frontal structure. Recently, *Browning et al.* [1998a] demonstrated how a combination of UHF and VHF profilers could delineate the mesoscale dynamics and structure of a cold front with unprecedented detail; and *Browning et al.* [1998b], using a VHF radar, presented an equally detailed study of a warm core cyclone that had developed from a hurricane remnant.

However, to fully exploit the VHF radar technique for mesoscale meteorology, a better understanding is required of the scattering mechanisms, in order to interpret the echo power profiles. In this paper we concentrate on echo powers from a vertically pointing radar beam. Two models have been presented in the literature for the scattering of VHF radiation by the clear atmosphere:

1. The Fresnel scatter model [*Gage et al.*, 1981] applies to the non turbulent atmosphere where the echo power decreases rapidly with zenith angle [*Gage and Green*, 1978]. It envisages that irregularities in refractive index on the vertical scale of half the radar wavelength are randomly distributed in the vertical but are coherent in the horizontal over scales greater than the radar's first Fresnel zone. As a consequence, the radar reflectivity η should follow

$$\eta = (\delta r)^2 \frac{F(\lambda)^2}{16} M^2, \qquad (1)$$

where δr is the range resolution of the radar, M is the vertical gradient of potential refractive index evaluated over a large scale (several hundred meters or more), and $F(\lambda)$ is a parameter relating refractive index variations on the small scale to the large-scale gradient. If the spectrum of variations in refractive index follows a universal shape, then F will be dependent only on the radar wavelength λ, and so the reflectivity will be proportional to M^2. M is defined as follows [*Ottersten*, 1969a]:

[1]Now at Cooperative Institute for Research in Environmental Science, University of Colorado, Boulder.

Paper number 1999RS002260.
0048-6604/00/1999RS002260$11.00

$$M = -77.6 \times 10^{-6} \frac{p}{T} \left(\frac{\partial \ln \theta}{\partial z} + \frac{15,500q}{T} \frac{\partial \ln \theta}{\partial z} - \frac{7750}{T} \frac{\partial q}{\partial z} \right), \quad (2)$$

where p, T, q, θ, and z are pressure, temperature, specific humidity, potential temperature, and height respectively.

2. The turbulent scatter model [*Ottersten*, 1969b] assumes active turbulence in the echo volume. The radar reflectivity is related to the refractive index structure constant c_n^2 and the radar wavelength λ by

$$\eta = 0.38 c_n^2 \lambda^{-1/3}. \quad (3)$$

Here c_n^2 may further be expressed as [*Doviak and Zrnic*, 1984, p. 403]

$$c_n^2 = a^2 \epsilon^{-1/3} K M^2, \quad (4)$$

where ϵ is the turbulent dissipation rate and K is the eddy diffusion coefficient. Here a^2 is a constant approximately equal to 3.3. Pure turbulent scatter is assumed to be isotropic: the reflectivity is constant with zenith angle.

These two models should be seen as limiting cases for the scattering mechanism, applicable in conditions of very high and very low anisotropy, respectively [*Röttger*, 1980]. (We define anisotropy in this paper as the ratio of echo power from the zenith and at 6° off vertical, expressed in decibels, following *Pepler et al.* [1998]. Both, however, predict that the echo power should be proportional to M^2. Empirical investigations comparing radar power to M^2 profiles derived from nearby radiosonde profiles in the upper troposphere and stratosphere uphold this hypothesis, at least in an average sense [*Gage et al.*, 1985; *Tsuda et al.*, 1988; *Vaughan et al.*, 1995]. The physical basis for the Fresnel scattering model was confirmed by balloon-borne observations of thin layers of enhanced stability in the stratosphere and upper troposphere [*Dalaudier et al.*, 1994], from which *Luce et al.* [1995] were able to synthesize a radar power profile in reasonable agreement with coincident VHF observations. Fresnel scatter therefore provides a good model for the scattering mechanism in the upper troposphere and lower stratosphere, particularly where the anisotropy is high.

Unfortunately, there has been less success in verifying the scattering models at lower levels. Here, the magnitude of M is dominated by the $\partial q/\partial z$ component [*Chu et al.*, 1990; *Luce et al.*, 1995]. Although Luce et al. did measure humidity on their balloon platforms, their instrument did not have the vertical resolution necessary to resolve meter-scale sheets. They could only relate the radar power measured to overall humidity gradients. Direct evidence for thin layers in humidity has so far only been found near the surface (*Muschinsky and Wode* [1998]; despite the title, this paper reported measurements from 200 to 600 m above the sea), but it is generally presumed that humidity structures analagous to those in temperature are responsible for VHF radar vertical echoes in the troposphere.

Tsuda et al. [1988] found that the M^2 model did not agree as well with radar measurements in the humidity-dominated region as it did above ~8 km. However, this study was based on just one radiosonde. A much more comprehensive study was conducted by *Chu et al.* [1990], who used four months' worth of radar data gathered for 2.5 hours each day with the Chung-Li (Taiwan) radar to compare with radiosondes launched 25 km away. By performing linear regression of echo power (in decibels) upon $\log_{10}(M^2)$ they found a reasonable correlation between the two quantities. However, the slope of the regression line varied considerably: in anticyclonic conditions it was generally in the range 1–1.8, but when a typhoon passed nearby, the slope was in the range 0.3–0.7. Lower slopes in the latter conditions were interpreted by the authors as evidence for a significant proportion of turbulent scatter in the measured signal. In fact, this variation in slope was also noticed by *Vaughan et al.* [1995] for comparisons between power and dry M^2 (evaluated without the humidity term) between 8 and 14 km, with a slope of 1 observed at low power and 0.65 at high power.

Mesosphere-stratosphere-troposphere radar echoes in the troposphere frequently show a complex pattern with layers of high and low echo power ascending or descending. An example from the Aberystwyth radar, discussed fully by *Browning et al.* [1998b], is shown in Figure 1. Here, the layer of high echo power which ascends from 3 to 8 km around 1430 UT marks a sharp negative-going humidity gradient at the top of the boundary layer. The radar's ability to track this layer enabled a detailed case study to be performed of the mesoscale structure of a warm core extratropical cyclone. Note the marked decrease in echo power throughout the troposphere from 1500 UT to 1730 UT. This was a period of heavy rain at the radar site, which is known to suppress VHF radar

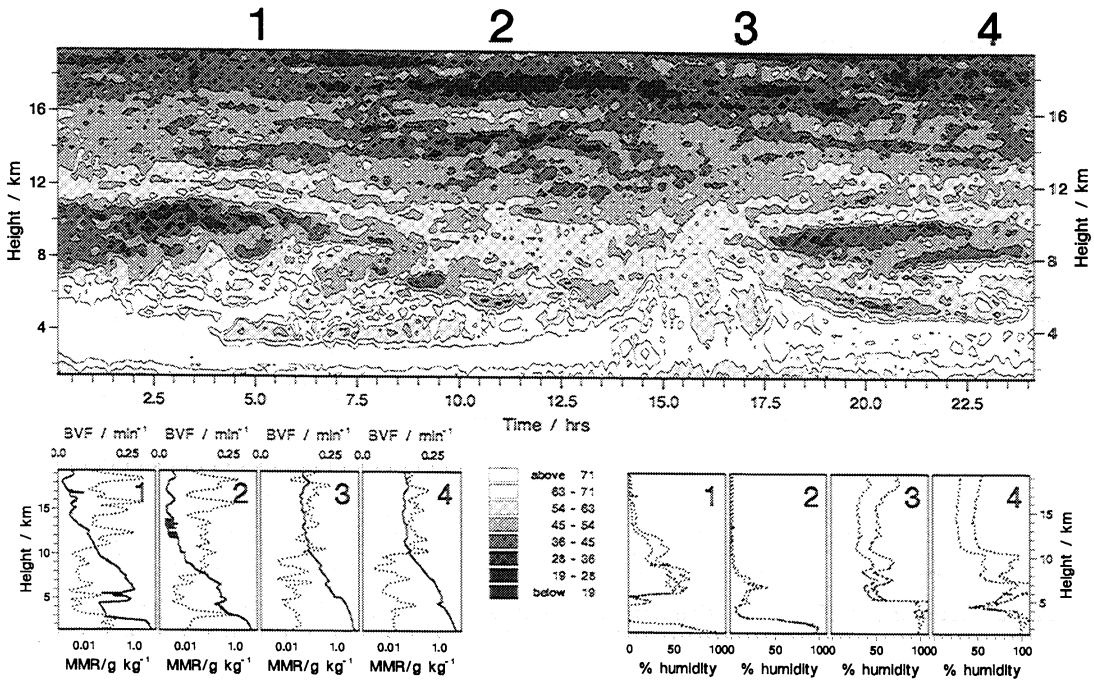

Figure 1. Height-time plot of radar vertical beam echo power from the Aberystwyth radar for October 28, 1996. Also shown are profiles of Brunt-Väisälä frequency (BVF, solid lines), water mass mixing ratio (MMR, dotted lines), and humidity relative to water and ice, measured by radiosondes at 0515, 1115, 1715, and 2315 UT. The radiosondes were launched from Aberporth, 50 km from the radar site.

echoes [*Chu and Lin*, 1994]. Indeed, in such conditions the radar echo contains a component from precipitation as well as clear air refractivity structures [*Fukao et al.*, 1985], which may be separated in the measured Doppler spectrum because of the fall speed of the large raindrops that contribute to the radar cross section (the volume reflectivity from precipitation is proportional to r^6, where r is the radius of the hydrometeor [*Doviak and Zrnic*, 1984]. *Chu et al.* [1990], *Chu and Lin* [1994], and *Chu and Song* [1998] showed that the precipitation echo at 50 MHz is generally weaker than that from the clear air, except near the melting level or bright band, where the precipitation echo is strongly enhanced (by ~10–15 dB). They also showed that the clear air echo is weaker in convective rainfall, a fact attributed by *Chu and Lin* [1994] to the effect of entrainment of dry, cold air into a warm, moist cloud: correlation of humidity and temperature fluctuations leads to lower values of M from (2).

In this paper we use data from the U.K. MST radar at Aberystwyth (52.4°N, 4.2°W) during January-March 1997, together with 300 radiosonde profiles measured from Aberporth (52.14°N, 4.57°W), 50 km from the radar site, to investigate further the applicability of (1) to explain vertical VHF echoes and, in particular, the effect of humidity on the echoes. The radar operates at 46.5 MHz, with peak power 120 kW and 5% duty cycle; a full description of it is given *Slater et al.* [1991]. For the observations presented here, the radar was operated with 8 μs pulses coded to 2 μs resolution (corresponding to 300 m in height). Vertical beam spectra were calculated by standard Fast Fourier Transform (FFT) techniques, using 64 points after coherent averaging of the signals for 0.167 s, giving a Nyquist frequency of 3 Hz. Measurements were made in the vertical and six off-vertical beams (four at 6° and one each at 4° and 8°), although this paper is concerned primarily with the vertical beam. The data analysis calculates the noise for each profile from the spectra in the uppermost height gates; thus signal power is correctly calculated for very broad spectra such as are sometimes seen in rain.

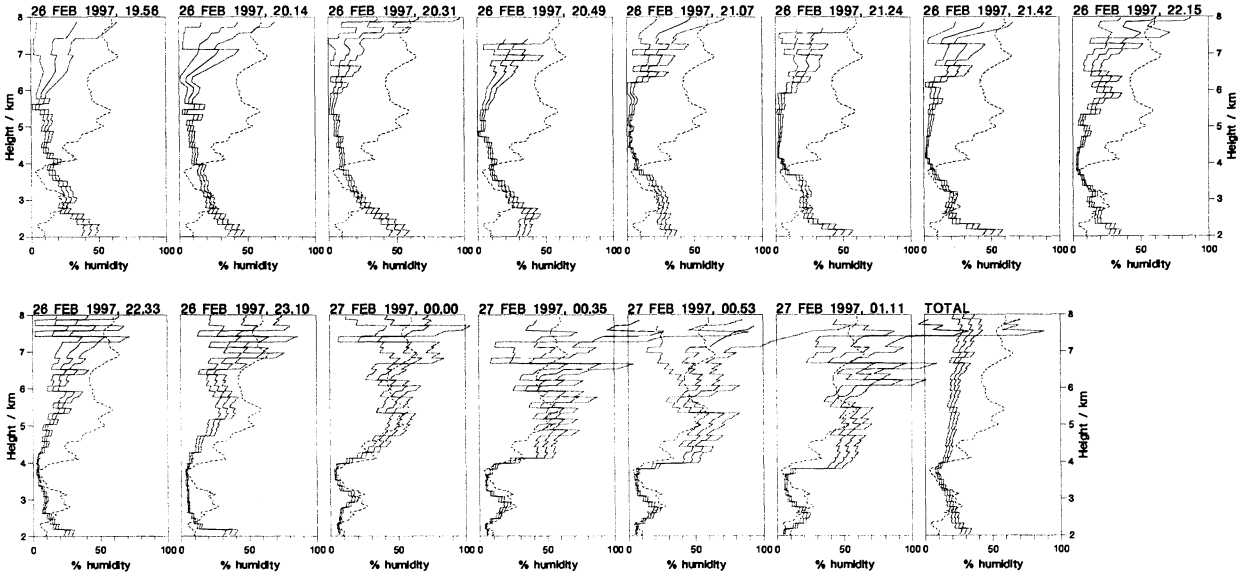

Figure 2. Comparison of lidar relative humidity profiles (solid lines with 1σ error bars) measured from 1956 UT, February 26, 1997 - 0111, February 27, 1997, with a sonde profile at 0000 UT (dashed lines). They agree only when the measurements are less than ~1 hour apart in time. The sonde temperature profile has been used to convert the mixing ratio profiles measured by the lidar to relative humidity.

2. Comparison Between Radar and Radiosondes

In order to verify that the humidity profiles measured at Aberporth can be taken as representative of the air over the radar, comparisons were conducted with a Raman water vapor lidar located only 2 km from the radar [*Vaughan et al.*, 1988]. Six nights' data were considered in the comparison. Figure 2 shows a typical example, with the lidar and sonde humidity profiles agreeing well, but only when the measurements are close in time. A similar conclusion was drawn from a comparison of radiosonde humidity from ascents at the two sites (radiosondes are flown

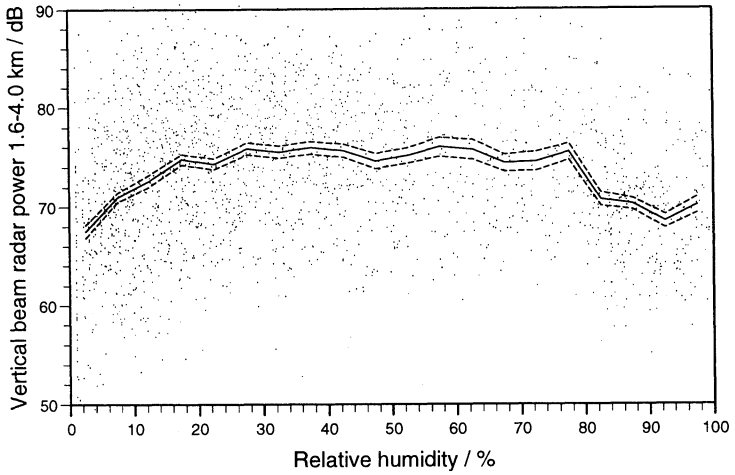

Figure 3. Dependence of radar power 3.0-4.0 km on relative humidity, measured by 300 sondes. Points are for individual 150 m layers, the solid and dashed lines are the average and standard error in the mean respectively of the points in each data bin of 5% relative humidity.

from Aberystwyth in conjunction with ozonesondes, but these profiles are far fewer in number than for the operational radiosondes). We therefore compare the radiosonde profiles with radar power averaged over 38 min in the same hour as the radiosonde. (Of course, the separation between the sonde and the radar will mean that there is on occasion a substantial difference in humidity between the two sites, but we expect such differences to be comparatively rare and to average out in the statistical study presented later, provided that orographic changes to q and dq/dz measured further inland by the sondes are negligible).

Looking at the effect of humidity alone, Figure 3 plots the dependence of echo power from 3–4 km altitude on relative humidity using 300 sondes available during January–March 1997. There is a large amount of scatter in the data, but the average values clearly show that the echo power tends to be weakest both in very dry and in very moist air.

A second example, Figure 4, shows the vertical echo power during February 17, 1997, together with the four radiosonde profiles measured at 0515, 1115, 1715, and 2315 UT. Echo power below 4 km is reduced by 5–10 dB from 0300 to 1750 UT, when sondes 1–3 indicate humidity near 100% through most of the troposphere. This is an example of the suppression of echo power in precipitation, as mentioned in section 1. On this day a frontal system crossed Aberystwyth, with stratiform precipitation, particularly in the morning when the warm front passed over. This shows that convective rainfall is not a precondition for reduced echo power, casting doubt on *Chu and Lin*'s [1994] hypothesis that the reduction results from entrainment and turbulent mixing by the convective clouds.

To compare the refractivity model quantitatively with the radar measurements, we exploit the result of *Vaughan et al.* [1995] that the two agree well in the stratosphere where the humidity term in (1) is negligible:

$$P \sim \frac{1}{z^2} M^2, \tag{5}$$

where P is radar power and z is altitude. Profiles of P were calculated from high-resolution (2 sec) radiosonde profiles by means of straight line fits over 600 m and fitted to observed radar power profiles in the stratosphere to determine the constant of proportionality in (2). Figure 5 shows two example profiles, one in unsaturated and one in saturated air. Above 3 km the M^2 model agrees reasonably well with observations in the unsaturated case, but it substan-

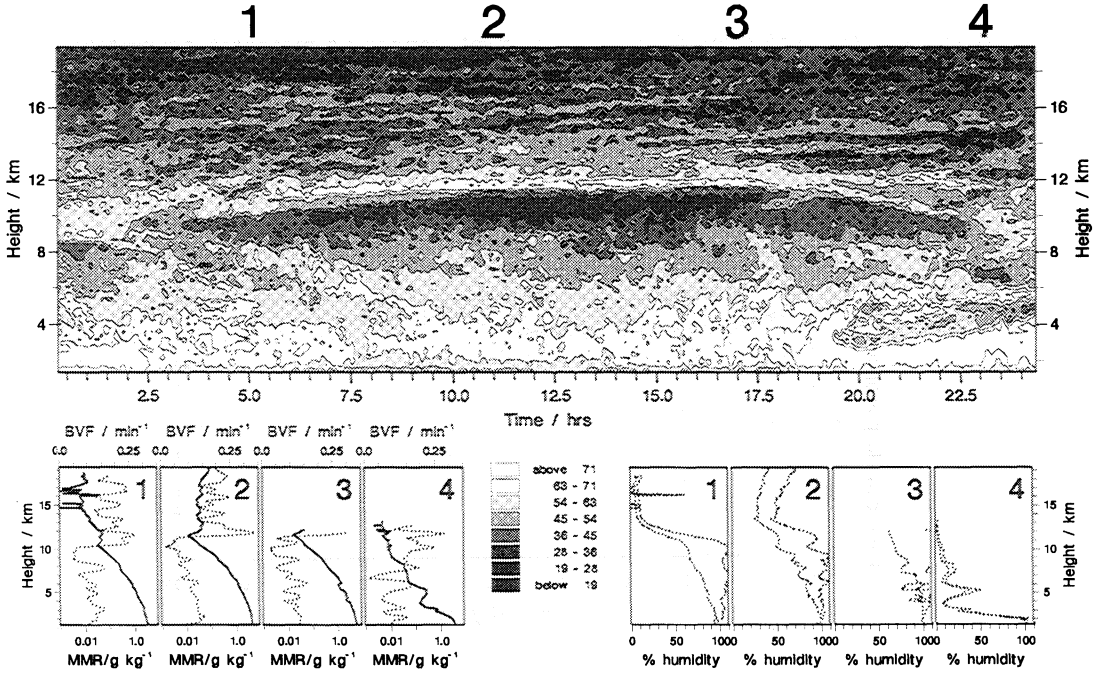

Figure 4. As in Figure 1, but showing reduced echo power in saturated air at the time of sondes 1-3.

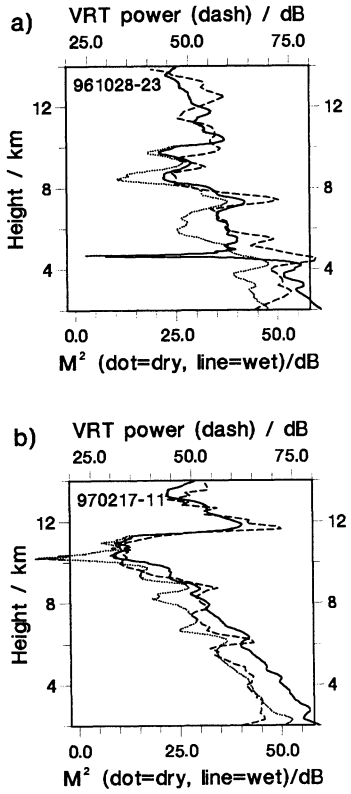

Figure 5. Example of a radar vertical beam echo profile (dashed lines) and model M^2 profiles including range correction, with and without the humidity contribution included (solid and dotted lines respectively). The plots use sonde 2 in Figure 4 and sonde 4 in Figure 1. a) unsaturated conditions; b) saturated conditions.

tially overpredicts the power in the saturated case: indeed,the profile of M^2 calculated with no humidity contribution provides a better fit to the data here! To illustrate this further, Fgure 6 shows the difference between the M^2 model and observations between 3 and 8 km from the entire data set.

We note first of all the considerable scatter of points in Figure 6. Part of this is likely to result from small differences in the altitudes of humidity and temperature gradients between Aberystwyth and Aberporth, to which the correlation method is particularly sensitive. Some will also be due to the empirical nature of the M^2 model itself: agreement between measurements and model should be expected in a statistical sense rather than in a deterministic fashion on each profile. Nevertheless, the mean model power shows interesting differences with observations: low for dry air (6–65% RH) and high for moist air (> 75%) with the greatest over estimate (4 dB) in saturated air.

The sonde humidity measurements may be unreliable, e.g., because of the response time and build up of ice on the sensor. However, eliminating all sonde profiles which passed through a low-level region with RH >90% gives no effect on the average curve for RH <90% in Figure 6. Rain in convective storms will be associated also with turbulent broadening of the echo spectra, which may become so broad that a Doppler peak cannot be measured accurately. For this reason, events where the vertical velocity measured by

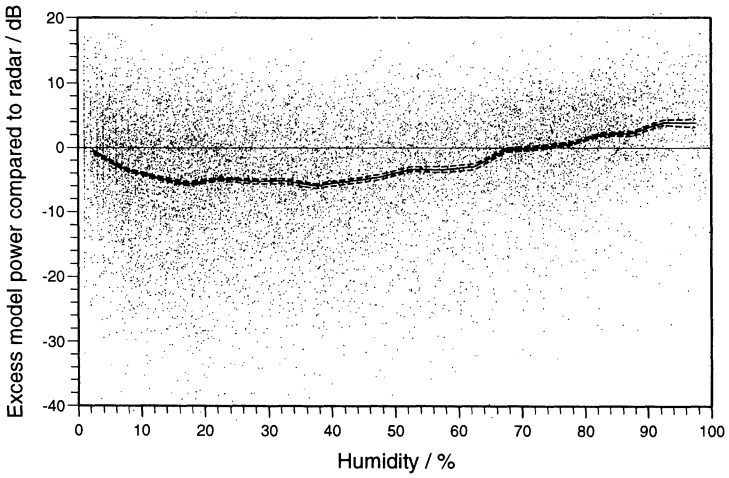

Figure 6. Difference between model and observed echo powers from 3 to 8 km as a function of the relative humidity, after fitting in the stratosphere. Points denote differences for individual 150 m layers; the solid and dashed lines are the average and standard error in the mean respectively of the points in each data bin of 5% relative humidity.

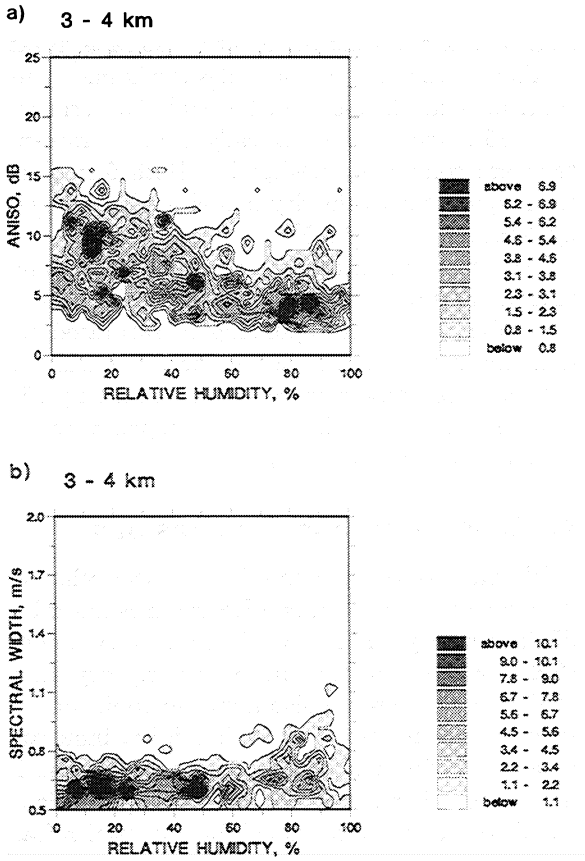

Figure 7. Scatter plot of a) anisotropy (dB), and b) spectral width (m/s), against relative humidity for vertical echo powers from the 3-4 km altitude range. Points have been aggregated into bins of 3% in RH, 1 dB in anisotropy and 0.05 m/s in spectral width. The shading represents the relative density of points.

the radar exceeded 1 ms^{-1} have been excluded from Figure 6 (although including them would not in fact make very much difference).

An indication that the scattering mechanism may be different in dry and moist air is provided by Figure 7, where the variation of spectral width and anisotropy is shown as a function of relative humidity for the layer between 3 and 4 km. At low humidity the anisotropy frequently exceeds 10 dB and spectral widths are small, consistent with Fresnel scatter. As humidity increases the anisotropy decreases and the spectral width increases, indicating a greater contribution from turbulent scatter.

3. Possible Explanation of Model Power Differences

There are two features of Figure 6 that require explanation: the apparent excess radar power over the model in the dry troposphere and the relatively low power in the moist troposphere. The model was fitted to the radar observations in the stratosphere, and the anomaly at low RH indicates a difference in the structure of small-scale refractivity anomalies between the stratosphere and troposphere. Briefly, it indicates that the troposphere is richer in small-scale anomalies relative to the overall M^2 gradient than the stratosphere. Since radar echoes in the troposphere tend to be dominated by the humidity terms, this is perhaps not surprising: it is simply saying that small-scale humidity gradients are distributed differently from those in potential temperature. Both kinds of gradient will be eroded equally by diffusion and mixing, whereas θ gradients will also be smoothed by radiative processes. We do not pursue this point further here but turn now to the second anomaly, that at high RH.

Differences between measurements and model at high humidity can be attributed to the effect of rain, if we accept that near-saturated air may recently have encountered rain. If rainfall has the effect of suppressing small-scale humidity fluctuations within the overall (saturated) humidity profile, then the fluctuations in refractive index which cause the radar echo will also be suppressed.

As an example of this, we now present a derivation of a saturated potential refractivity, applicable to a completely saturated atmosphere. We follow closely the derivation of M^2 by *Ottersten* [1969a], but instead of applying conservation of potential temperature and absolute humidity to air parcels displaced vertically, we apply conservation of wet bulb potential temperature: i.e., displacement along the saturated rather than dry adiabatic.

Consider a reference level z_0, where the pressure, temperature, and vapor pressure are p_0, T_0, and e_0. Now consider a parcel of air displaced (down) from z_1 to z_0 where $z_1 - z_0 = \Delta z > 0$. Let

$$N = \frac{Ap}{T} + \frac{ABe}{T^2} \tag{6}$$

be the refractive index of the air minus 1, where A = 77.6 $\times 10^{-6}$ and B = 4810 [*Doviak and Zrnic*, 1984]. The displaced parcel attains values of T_2 and e_2 at

z_0 (p equalizes immediately, so $p_2 = p_0$) and hence has refractive index N_2. Then M is represented by

$$M = \frac{N_2 - N_0}{\Delta z} = \frac{\partial N}{\partial T}\frac{(T_2 - T_0)}{\Delta z} + \frac{\partial N}{\partial e}\frac{(e_2 - e_0)}{\Delta z}. \quad (7)$$

1. In the unsaturated case, T_2 adjusts along the dry adiabatic Γ_d, and the mass mixing ratio q_1 is conserved. So

$$T_2 = T_1 + \Gamma_d \Delta z \quad and \quad e_2 = \frac{q_1 p_0}{\epsilon}, \quad (8)$$

where $\epsilon = 0.622$ converts between mass and volume mixing ratio. Therefore, taking the limit $\Delta z \to 0$,

$$M = \frac{\partial N}{\partial T}\left(\frac{\partial T}{\partial z} + \Gamma_d\right) + \frac{\partial N}{\partial e}\frac{p}{\epsilon}\frac{\partial q}{\partial z} \quad (9)$$

$$M = \frac{T}{\theta}\frac{\partial \theta}{\partial z}\frac{\partial N}{\partial T} + \frac{\partial N}{\partial e}\frac{p}{\epsilon}\frac{\partial q}{\partial z} \quad (10)$$

from which the formula of *Ottersten* [1969a] already quoted as (2) is readily derived.

2. In the saturated case, e_0, e_1, and e_2 are all simply functions of temperature. In this case,

$$T_2 = T_1 + \Gamma_s \Delta z, \quad (11)$$

where Γ_s is the saturated lapse rate. So, writing $e_s(T)$ for the saturation vapor pressure at T,

$$e_2 = e_0 + \frac{de_s}{dT}(T_2 - T_0), \quad (12)$$

$$e_2 - e_0 = \frac{de_s}{dT}\left(\frac{\partial T}{\partial z} + \Gamma_s\right)\Delta z, \quad (13)$$

$$M = \left(\frac{\partial N}{\partial T} + \frac{\partial N}{\partial e}\frac{de_s}{dT}\right)\left(\frac{\partial T}{\partial z} + \Gamma_s\right), \quad (14)$$

$$M = -\frac{Ap}{T^2}\left(1 + \frac{2q_s B}{\epsilon T} - \frac{BLq_s}{\epsilon r' T^2}\right)\left(\frac{\partial T}{\partial z} + \Gamma_s\right), \quad (15)$$

using the Clausius-Clapeyron equation for de_s/dT. Here, q_s is the saturated mixing ratio, L is the latent hear of vaporization of water, and r' is the gas constant for water vapor.

This model predicts far lower echo power than the standard model: indeed, at some height in the troposphere it is almost certain to predict zero power. At low level the first bracket is dominated by the third term and so is negative, giving a positive value of M. (At ground level, $M > 0$ for T > 263.5 K.) In the upper troposphere the terms containing q_s become very small and the bracket reduces to 1, so M is negative.

Above ~10 km in midlatitudes the humidity terms contribute much less than the stability term to (2) and (15), and in the statically stable stratosphere they are completely negligible. Both formulae are then equivalent to the dry model used, for instance, by *Vaughan et al.* [1995].

Using the same fitting constant as for the standard model, the predictions of (11) were compared with the radar power corresponding to saturated conditions measured by the radiosondes. For RH > 90% the measured power exceeded the model by 15 dB, substantially more than the discrepancy with the standard model (Figure 6).

4. Discussion and Conclusions

We have shown (Figure 3) that the echo power from a vertically pointing VHF radar is lower by ~5 dB in very dry air (RH < 10%) and very humid air (RH > 85%) than that in moderately dry air (30–70%). The echoes are also more isotropic, and their spectra are broader, at high humidity, indicating a greater contribution from turbulent rather than Fresnel scatter. Further, when the radar power is compared to the standard model for potential refractivity (equation (2)) after fitting in the stratosphere, the model is found to under predict the power by ~6 dB at moderate humidity and to overpredict by ~4 dB near saturation. Episodes of heavy rain lead to further suppression of the echo power (e.g., Figure 1).

A possible cause for the suppression of radar power at high humidity is the effect of precipitation. It is already known from *Chu et al.* [1990], *Chu and Lin* [1994], and *Chu and Song* [1998] that precipitation suppresses clear air radar echoes. However, the mechanism they proposed for this suppression depended on convective entrainment and should not operate in layer clouds as in the February 17 1997 case (Figure 4). It is not clear either how the effects of the entrainment would persist in moist, but unsaturated, air as is clearly shown in Figures 3 and 6. We suggest here an alternative mechanism, essentially proposing that heavy rain acts as a source of moisture which tends to "wash out" small-scale irregularities in humidity, bringing the air to the local saturated vapor pressure. Irregularities in humidity and temperature will then be necessarily correlated. Air that has been so processed will take time to build up a full spectrum of irregularities again, so the ef-

fects of precipitation will persist even when the rain or snow has ceased. In an attempt to construct a quantitative model of these effects we have rederived *Ottersten*'s [1969a] formula assuming perfect saturation. When compared with the radar measurements in near-saturated air, this predicts ~20 dB less power than observed (i.e., ~25 dB less than equation 1).

The conditions under which (15) is valid are a limiting case, unlikely to be observed consistently in the atmosphere. These conditions imply that the vapor pressure in a turbulent patch equilibrates immediately to small changes in temperature. Diffusion of water vapor to and from raindrops will limit the efficiency of this process and introduce a lag between fluctuations in q and those in temperature. The rigid coupling between temperature and humidity fluctuations implied by (15) will not therefore occur in practice. Nevertheless, the model is not without value: some modification of the small-scale refractivity structure by rainfall is inevitable, and the model predicts the sign and limiting magnitude of this effect.

We conclude that a re-examination of *Ottersten*'s [1969a] formula helps to illuminate the physics responsible for the suppression of VHF echo power at high humidity and propose that these differences are basically caused by a suppression of small-scale refractivity structures by falling precipitation. Further work is needed to examine this hypothesis more rigorously: for example, rainfall rate measurements are required at the radar site to enable periods of and intensity of precipitation to be unambiguously identified.

Acknowledgments. We thank Ken Gage and an anonymous referee for useful comments on the first manuscript of this paper. The Aberystwyth MST radar is a NERC national facility. Data were supplied by the British Atmospheric Data Centre, including radiosonde data from the U.K. Meteorological Office. We acknowledge the financial support of NERC for this project.

References

Browning, K.A., D. Jerrett, J. Nash, T. Oakley, and N.M. Roberts, Cold frontal structure derived from radar wind profiles, *Meteorol. Appl., 5*, 67–74, 1998a.

Browning, K.A., G. Vaughan, and P. Panagi, Analysis of an ex-tropical cyclone after re-intensifying as a warm core extra-tropical cyclone, *Q. J. R. Meteorol. Soc., 124*, 2329–2356, 1998b.

Chu, Y.-H. and C.-H. Lin, The severe depletion of turbulent echo power in precipitation observed using the Chung-Li VHF Doppler radar, *Radio Sci., 29*, 1311–1320, 1994.

Chu, Y.-H., and J.S. Song, Observation of precipitation associated with a cold front using a VHF wind profiler and a ground-based optical rain gauge, *J. Geophys. Res., 103*, 11,401–11,409, 1998.

Chu, Y.-H., T.S. Hsu, L.H. Chen, J.K. Chao, C.H. Liu, and J. Röttger, A study of the characteristics of VHF radar echo power in the Taiwan area, *Radio Sci., 25*, 527–538, 1990.

Dalaudier, F., C. Sidi, M. Crochet, and J. Vernin, Direct evidence of "sheets" in the atmospheric temperature field, *J. Atmos. Sci., 51*, 237–248, 1994.

Doviak, R.J. and D.S. Zrnic, *Doppler Radar and Weather Observations*, Academic, San Diego, Calif., 1984.

Fukao, S.K., K. Wakasugi, T. Sato, S. Morimoto, T. Tsuda, I. Hirota, I. Kimura, and S. Kato, Direct measurement of air and precipitation particle motion by VHF Doppler radar, *Nature, 316*, 712–714, 1985.

Gage, K.S., and J.L. Green, Evidence for specular reflection from monostatic VHF radar observations of the stratosphere, *Radio Sci., 13*, 991–1001, 1978.

Gage, K. S., B. B. Balsley, and J. L. Green, Fresnel scattering model for the specular echoes observed by VHF radar, *Radio Sci., 16*, 1447-1453, 1981.

Gage, K.S., W.L. Ecklund, and B.B. Balsley, A modified Fresnel scattering model for the parametrization of Fresnel returns, *Radio Sci., 20*, 1493–1501, 1985.

Larsen, M.F., and J. Röttger, Observations of frontal zone and tropopause structures with a VHF Doppler radar and radiosondes, *Radio Sci., 20*, 1223–1232, 1985.

Luce, H., M. Crochet, F. Dalaudier, and C. Sidi, Interpretation of VHF ST radar vertical echoes from in-situ temperature sheet observations, *Radio Sci., 30*, 1003-1025, 1995.

May, P.T., M. Yamamoto, S. Fukao, T. Sato, S. Kato, and T. Tsuda, Wind and reflectivity fields around fronts observed with a VHF radar, *Radio Sci., 26*, 1245–1249, 1991.

Muschinski, A., and C. Wode, First in-situ evidence for co-existing submeter temperature and humidity sheets in the lower free troposphere, *J. Atmos Sci., 55*, 2893–2906, 1998.

Ottersten, H., Mean vertical gradient of potential refractive index in turbulent mixing and radar detection of CAT, *Radio Sci., 4*, 1247–1249, 1969a.

Ottersten, H., Radar backscattering from the turbulent clear atmosphere, *Radio Sci., 4*, 1251-1255, 1969b.

Pepler, S. J., G. Vaughan, and D. A. Hooper, Detection of turbulence around jet streams using a VHF radar, *Q. J. R. Meteorol. Soc., 124*, 447-462, 1998.

Röttger, J., VHF radar observations of a frontal passage, *J. Appl. Meteorol., 18*, 85–91, 1979.

Röttger, J., Reflection and scattering of VHF radar signals from atmospheric refractivity structures, *Radio Sci., 15*, 259-276, 1980.

Shapiro, M.A., T. Hample, and D.W. Van de Kamp, Radar wind profiler observations of fronts and jet streams, *Mon. Weather Rev., 112*, 1263–1266, 1984.

Slater, K., A. D. Stevens, S. A. M. Pearmain, D. Eccles,

A. J. Hall, R. G. T. Bennett, L. France, G. Roberts, Z. K. Olewicz, and L. Thomas, Overview of the MST radar system at Aberystwyth, in *Proceedings of the Fifth Workshop on Technical and Scientific Aspects of MST Radar*, pp. 479-482, SCOSTEP secretariat, Univ. of Ill., Urbana,1991.

Tsuda, T., P.T. May, T. Sato, S. Kato, and S. Fukao, Simultaneous observations of reflection echoes and refractive index gradient in the troposphere and lower stratosphere, *Radio Sci., 23*, 655–665, 1988.

Vaughan, G., D. P. Wareing, L. Thomas, and V. Mitev, Humidity measurements in the free troposphere using Raman backscatter, *Q. J. R. Meteorol. Soc., 114*, 1471-1484, 1988.

Vaughan, G., A. Howells, and J.D. Price, Use of MST radars to probe the mesoscale structure of the tropopause, *Tellus Ser.#A, 47*, 759–765, 1995.

G. Vaughan, Department of Physics, University of Wales, Aberystwyth, Aberystwyth, Ceredigion SY23 3BZ, Wales, U. K. (gxv@aber.ac.uk)

R. M. Worthington, CIRES, University of Colorado, Boulder, Co 80309-0216

(Received September 28, 1999; revised June 19, 2000; accepted June 21, 2000.)